Anisotropic Meta-substrate Conical-Beam Leaky-Wave Antenna

Attieh Shahvarpour [#1], Alejandro Alvarez Melcon [*2], Christophe Caloz [#3]

[#]*Electrical Engineering Department, École Polytechnique de Montréal*
Poly-Grames Research Center, 2500, Chemin Polytechnique, Montréal, QC, H3T 1J4
[1]attieh.shahvarpour@polymtl.ca
[3]christophe.caloz@polymtl.ca

[*]*Electrical Engineering Department, Universidad Politécnica de Cartagena*
Campus Muralla del Mar-Antiguones, 30202 Cartagena (Murcia), Spain
[2]alejandro.alvarez@upct.es

***Abstract*— A broadband and low beam squint anisotropic magneto-dielectric 2D leaky-wave antenna excited by a vertical electric source is presented. A comparison of the TM$_z$ dispersion behavior of the structure for Drude/Lorentz dispersive anisotropic and an isotropic non-dispersive grounded slabs is performed. The isotropic slab is restricted to leaky-wave pointing angles near endfire with very low radiation performance due to the inherent endfire radiation null caused by the slab. As a result, its radiation is dominated by the space-wave, which leads to low directivity and beam scanning incapability. In contrast, the anisotropic meta-substrate provides a highly directive and efficient 2D leaky-wave radiation with great design flexibility. At its lower frequencies, it provides narrow-band full-space conical-beam scanning while at higher frequencies, it enables a designable angle fixed-beam with low-beam squint radiation. This antenna may find applications in broadband point-to-point communication and radar systems.**

I. Introduction

Leaky-wave antennas, which are characterized by high directivity and frequency beam scanning capability, have found wide applications in radar, point-to-point communications and MIMO systems. 2D leaky-wave antennas excited in their center feature a conical-beam radiation pattern as a result of cylindrical wave propagation outward from the source along the structure [1]. Several 2D leaky-wave antennas have been reported in the past, including periodic partially reflective screen [2], dielectric superstrate [3] and metamaterial [4]-[6] structures.

In this paper, a 2D leaky-wave antenna constituted of a uniaxially anisotropic meta-substrate excited by a vertical electric point source is proposed and analyzed by the spectral domain equivalent transmission line approach. The substrate is assumed to exhibit a Drude dispersive permittivity along the axis perpendicular to its plane and a Lorentz permeability in the plane of the substrate. Such a substrate may be implemented with a mushroom-type structure [5], [7] and [8], where the Drude dispersive permittivity is provided by the metal vias and the Lorentz dispersive permeability is provided by the metal rings formed by adjacent vias in the plane of the substrate. It is shown that this structure implements a 2D leaky-wave antenna which can support broadband, highly directive and low beam squint leaky-wave radiation in the right-handed (RH) region of the medium dispersion diagram, in contrast to isotropic structures (conventional dielectric).

The paper first compares the TM dispersion properties of the Drude/Lorentz dispersive anisotropic and isotropic non-dispersive grounded slabs. A vertical point source for the excitation of the TM leaky modes is then introduced and the asymptotic far-field radiation patterns are computed from the Green's functions using the transmission line model of the structure [9].

II. Definition of the Medium

The anisotropic meta-substrate is shown in Fig. 1 along with the TM$_z$ field configuration. The medium is defined by the permittivity and permeability tensors

$$\bar{\bar{\varepsilon}} = \begin{pmatrix} \varepsilon_\rho & 0 & 0 \\ 0 & \varepsilon_\rho & 0 \\ 0 & 0 & \varepsilon_z \end{pmatrix}, \quad \bar{\bar{\mu}} = \begin{pmatrix} \mu_\rho & 0 & 0 \\ 0 & \mu_\rho & 0 \\ 0 & 0 & \mu_z \end{pmatrix}. \qquad (1)$$

In typical meta-substrates such as the mushroom-type structure with the vias directed along z, the implants affect ε_z and μ_ρ, while ε_ρ and μ_z remain the same as those of the host medium (e.g. teflon) [8]. Typically, the host medium and therefore ε_ρ and μ_z are non-dispersive, while ε_z and μ_ρ exhibit dispersive characteristics due to the implants. In the frequency range where the vias of the mushroom-type structure are electrically short or densely packed [10], the effective permittivity term ε_z is modeled by the local Drude dispersion expression [11]

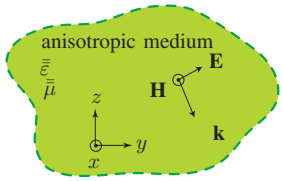

Fig. 1: Effective uniaxial anisotropic medium characterized by the permittivity and permeability tensors of Eq. (1), along with the TM$_z$ field configuration.

$$\frac{\varepsilon_z}{\varepsilon_0} = \varepsilon_{r\infty}\left[1 - \frac{{\omega_{pe}}^2}{\omega^2 - j\omega\zeta_e}\right], \qquad (2)$$

where $\varepsilon_{r\infty}$ and ω_{pe} are the host medium permittivity, and the electric plasma frequency, respectively, and ζ_e is the dissipation factor. The effective permeability μ_ρ which is related to the rings between the adjacent vias is modeled by the magnetic Lorentz dispersion relation [12]

$$\frac{\mu_\rho}{\mu_0} = 1 - \frac{F\omega^2}{\omega^2 - {\omega_{m0}}^2 - j\omega\zeta_m}, \tag{3}$$

where F is a factor related to the geometry of the current loops, ω_{m0} is the resonant frequency of these loops, $\omega_{pm} = \omega_{m0}/\sqrt{1-F}$ is the plasma frequency and ζ_m is the dissipation factor.

III. Dispersion Analysis

Fig. 2a shows the anisotropic meta-substrate of interest. The TM_z dispersion relation of the structure is derived by the transverse resonance technique [13] using the meta-substrate source-less transmission line model [14] shown in Fig. 2b as follows [15]

$$jZ_c \tan(\beta d) + Z_{c0} = 0, \tag{4}$$

where $\beta = \pm\sqrt{\omega^2\mu_\rho\varepsilon_z - {k_\rho}^2}\sqrt{\varepsilon_\rho/\varepsilon_z}$ and $Z_c = \pm\sqrt{\omega^2\mu_\rho\varepsilon_z - {k_\rho}^2}/(\omega\varepsilon_\rho)\sqrt{\varepsilon_\rho/\varepsilon_z}$ are the TM_z phase constant along the z axis and the characteristic impedance of the line, respectively, and $Z_{c0} = k_{z0}/\omega\varepsilon_0$ is the TM_z free-space characteristic impedance, where $k_{z0} = \mathrm{Re}(k_{z0}) + j\mathrm{Im}(k_{z0})$ is the TM_z free-space wave number along z. The dispersion relation of Eq. (4) is transcendental. The k_ρ dispersion curves are obtained numerically by computing its roots versus frequency. The permittivity and permeability dispersion curves

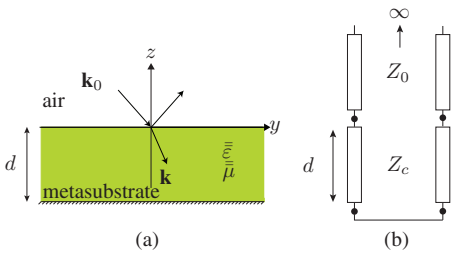

Fig. 2: Uniaxially anisotropic grounded slab and its transmission line model. (a) TM_z waves incident onto the slab. (b) Transmission line model (source-less case).

[Eqs. (2) and (3)] are plotted in Fig. 3 for the parameters given in the caption of the figure. The value ω_p ($f = 11$ GHz) was chosen so that the leaky-wave cutoff frequency of the anisotropic slab occurs at the same frequency as that for the isotropic non-dispersive one. The TM_z dispersion curves of the anisotropic meta-substrate with the medium dispersion of Fig. 3 are shown in Fig. 4, and are compared with the isotropic non-dispersive slab. This figure shows that a sufficient uniaxial anisotropy transforms surface modes into leaky modes over a very broad bandwidth. The reason for this behavior is the fact that the effective refractive index $n_e = \sqrt{\varepsilon_z\mu_\rho}/\sqrt{\varepsilon_0\mu_0}$ remains always smaller than 1, due to the asymptotic behavior

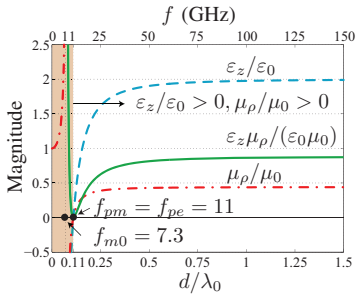

Fig. 3: Dispersive response for the permittivity $\varepsilon_z/\varepsilon_0$ (Drude model) and permeability μ_ρ/μ_0 (Lorentz model) with $\omega_{pe} = \omega_{pm}$. The parameters are: $F = 0.56$, $\omega_{m0} = 2\pi \times 7.3 \times 10^9$ rad/s, $\omega_{pm} = \omega_{m0}/\sqrt{1-F} = 2\pi \times 11 \times 10^9$ rad/s, $\varepsilon_{r\infty} = 2$, and $\zeta_e = \zeta_m = 0$. The substrate thickness is $d = 3$ mm.

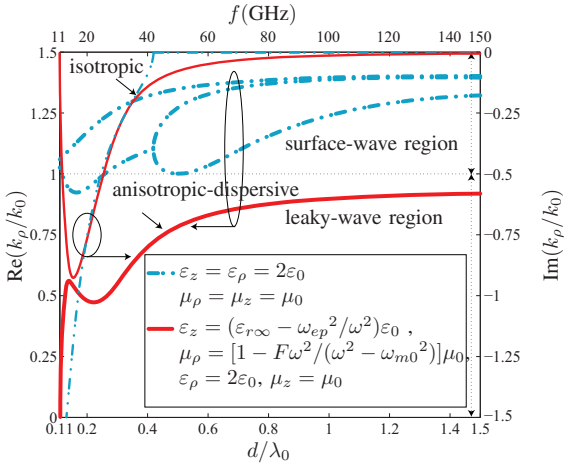

Fig. 4: Comparison of the dispersions of the first TM_z leaky modes for non-dispersive isotropic ($\varepsilon_z = \varepsilon_\rho = 2\varepsilon_0, \mu_\rho = \mu_z = \mu_0$) and dispersive anisotropic ($\varepsilon_z = \varepsilon_{r\infty}(1 - {\omega_{ep}}^2/\omega^2)\varepsilon_0$, $\varepsilon_\rho = 2\varepsilon_0$, $\mu_\rho = [1 - F\omega^2/(\omega^2 - {\omega_{m0}}^2)]\mu_0$, $\mu_z = \mu_0$). The non specified parameters are the same as Fig. 3.

of μ_ρ, $\mu_\rho(\omega \to \infty) = 1 - F < 1$ (for a relatively small host medium permittivity $\varepsilon_{r\infty}$). Due to this behavior, the propagation angle in the slab with respect to the normal to the interface remains always smaller than the critical angle, and therefore always leaks out. The dispersion-less response achieved at high frequencies is due to the fact that as frequency increases, the angle of propagation inside the substrate with respect to the normal to the interface progressively increases so that $k_\rho \to k_0$.

IV. Far-Field Radiation Analysis

A. Vertical Point Source Green's Functions

For the excitation of the TM_z modes a spectral domain vertical point source $\tilde{\mathbf{J}} = 1/(2\pi)\delta(z - z')\mathbf{a}_z$ embedded in the meta-substrate is used, as shown in Fig. 5a. The corresponding equivalent transmission line model is shown in Fig. 5b, where the vertical point source is modeled by the series voltage source $V_g = |\tilde{\mathbf{J}}| = J_z$ [16]. Using Sommerfeld's choice for the potentials [9], the far fields can be determined by the $\tilde{G}_A^{zz}$ component of the spectral-domain magnetic vector potential Green's function $\bar{\bar{\tilde{G}}}_A$. By substituting Eq. (1) into the spectral-domain Maxwell's equations with the source $\tilde{\mathbf{J}}$

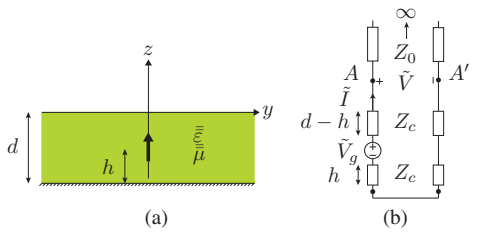

Fig. 5: Uniaxially anisotropic grounded slab excited by an embedded vertical point source. (a) Physical structure. (b) Transmission line model.

and manipulating the resulting relations, from the equivalent transmission line equations we obtain

$$\tilde{G}_A^{zz} = \frac{-j\mu_\rho}{\omega\varepsilon_z}\tilde{I}, \tag{5}$$

where $\tilde{I}$ is the spectral domain current along the equivalent transmission line. This expression can be easily reduced to the Green's function of an isotropic slab [16].

B. Asymptotic Far-Field Expressions

The far field radiation from a z-directed source in a layered medium may be calculated by the corresponding Green's functions $[\tilde{G}_A^{zz}(k_x,k_y)]$ at the interface with air (at AA' in Fig. 5b) as $\tilde{g}_A^{zz}(k_x,k_y,z) = \tilde{G}_A^{zz}(k_x,k_y,z=d)\exp(-jk_{z0}z)$. The double Fourier transformation relating the spectral to the spatial domain Green's function reduces then to the value of the integrand at the saddle point [14], [17] and [18], resulting in

$$g_A^{zz}(k_x,k_y,z) = jk_0\cos\theta\tilde{G}_A^{zz}(k_x,k_y)\frac{\exp(-jk_0r)}{r}. \tag{6}$$

The electric field is then calculated from Eq. (6) as $\mathbf{E}(x,y,z) = -j\omega\bar{\bar{\mathbf{g}}}_A(x,y,z)\cdot\mathbf{a}_z = -j\omega g_A^{zz}(x,y,z)\mathbf{a}_z$ [9]. Since $E_\theta(x,y,z)\mathbf{a}_\theta = -E_z(x,y,z)\sin\theta\mathbf{a}_z$, we finally obtain

$$E_\theta(x,y,z) = \frac{-1}{2}\omega k_0\sin(2\theta)\tilde{G}_A^{zz}(k_x,k_y)\frac{\exp(-jk_0r)}{r}. \tag{7}$$

V. Comparison of the Performance of the Isotropic and Double Anisotropic Structures

The isotropic grounded slab suffers of very low performance as a 2D leaky-wave antenna for the following reasons. i) Its leaky-wave pointing angle θ_p is limited to a narrow angular range near endfire ($68^\circ - 90^\circ$ in Fig. 6a), which is not desired in planar antenna applications where radiation close to broadside is generally required (e.g. flush-mounted antennas with obstacles in the plane of the antenna). This limitation is related, via the scanning law $\theta_p \simeq \sin^{-1}(\beta_\rho/k_0)$ [1], to the fact that the phase constant β_ρ cannot reach values significantly smaller than k_0 (Fig. 6a). ii) Because of the effect of the slab, the far-field pattern has a null at endfire, as shown by the $\cos\theta$ factor in Eq. (6). This null tries to annihilate the radiation of the leaky wave, which as already mentioned, occurs only near endfire. As a consequence the radiation is dominated by the space wave, whose beam direction is related to the electrical thickness of the substrate. Fig. 7 shows the radiation patterns for the isotropic slab for various frequencies on the leaky-wave

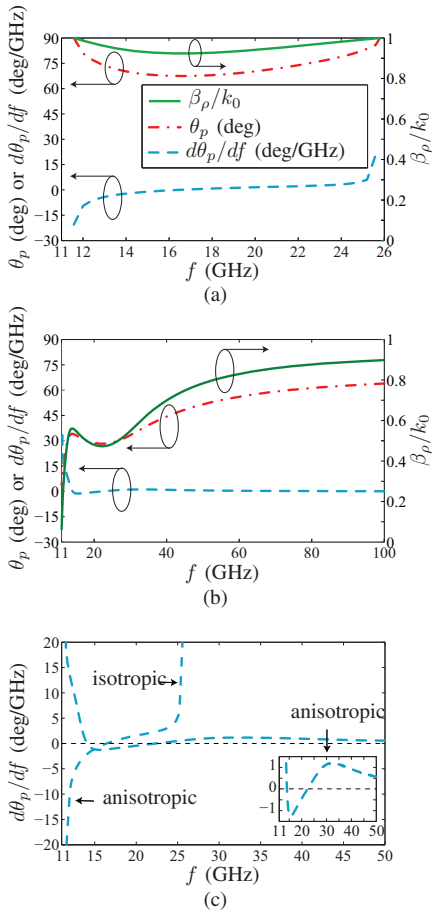

Fig. 6: Pointing angle of the leaky mode ($\theta_p = \sin^{-1}(\beta_\rho/k_0)$ [1]) and its variations over the frequency for the slab with the dispersion curves of Fig. 4 and $d = 3$ mm. (a) Isotropic slab with $\varepsilon_z = \varepsilon_\rho = 2\varepsilon_0$, $\mu_\rho = \mu_z = \mu_0$. (b) Anisotropic slab with $\varepsilon_z = \varepsilon_{r\infty}(1 - \omega_{pe}{}^2/\omega^2)\varepsilon_0$, $\varepsilon_\rho = 2\varepsilon_0$, $\mu_\rho = [1 - F\omega^2/(\omega^2 - \omega_{m0}{}^2)]\mu_0$, $\mu_z = \mu_0$. (c) Comparison of the variations of the pointing angle with respect to frequency for the isotropic and anisotropic substrates.

dispersion curve of Fig. 6a and at one non-physical frequency, where the leaky wave cannot propagate (Fig. 4). Fig. 7 shows that the angles of radiation at these frequencies point at around $\theta = 45^\circ$, which does not correspond to the angles predicted by the leaky-wave scanning law in Fig. 6a and are almost close to the radiation at 27 GHz (no leaky-wave radiation). Therefore, the radiation is not due to the leaky wave but to the space wave which does not allow scanning and provides little radiation directivity. iii) The radiation efficiency (both for the leaky and space waves) is reduced by the propagation the first surface mode (TM_0) (Fig. 4), since it carries part of the energy of the source in the slab.

In contrast, the double anisotropic meta-substrate exhibits high leaky-wave antenna performance, for the following reasons. i) The antenna is capable to radiate in a wide range of beam pointing angles, from broadside almost to endfire (0° to 65°, as shown in Fig. 6b). The reason for this behavior is understood from Fig. 3, where $0 \leq \varepsilon_z\mu_\rho/(\varepsilon_0\mu_0) < 1$, and therefore $0 \leq \beta_\rho/k_0 < 1$. Fig. 8 shows the scanning behavior of the leaky-wave antenna over the broad frequency range of 11 GHz to 100 GHz. Due to the vertical orientation of the

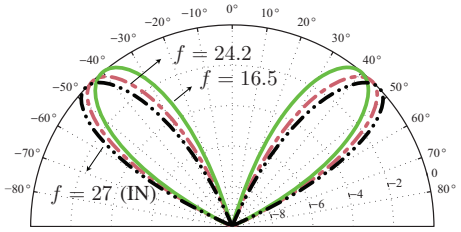

Fig. 7: Radiation from the isotropic grounded slab for various frequencies of Fig. 6a and for the frequency of $f = 27$ GHz, which is in the improper non-physical (IN) region of the dispersion curve of Fig. 4. The unit for the indicated frequencies is GHz.

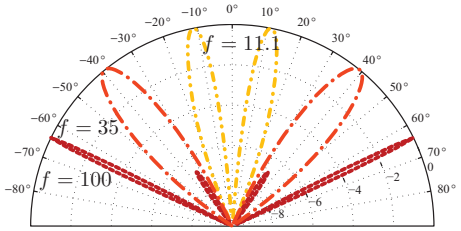

Fig. 8: Scanning behavior of the double anisotropic antenna in a wide band frequency range. The indicated frequencies are in GHz

point source excitation, there is always a null in the radiation pattern in the broadside direction. ii) The radiation efficiency of the meta-substrate leaky-wave antenna is much higher than that for the isotropic structure, as no surface modes exist in the leaky-mode frequency range ($0 \leq \varepsilon_z\mu_\rho/(\varepsilon_0\mu_0) < 1$), as shown Fig. 4. Therefore no energy is stored inside the dielectric through the surface modes. iii) The bandwidth of the leaky mode is wider than that for the isotropic structure, as shown in Fig. 4. In Fig. 3 $\lim_{\omega\to\infty} \varepsilon_z\mu_\rho/(\varepsilon_0\mu_0) < 1$ in the right-handed frequency range which leads to a wide frequency band of operation. The fundamental reason for this large bandwidth is the asymptotic $\mu_\rho < 1$ behavior of the Lorentz permeability (Fig. 3), which makes the effective refractive index $n_e = \sqrt{\varepsilon_z\mu_\rho}/\sqrt{\varepsilon_0\mu_0}$ of the slab smaller than that of air, $n_e < 1$, (assuming a reasonably low ε_z), in a wide band frequency range in contrast to the case of the isotropic slab ($n_e > 1$). iv) The beam squinting is extremely low as a consequence of the previous point. Fig. 6c compares the beam squinting $d\theta_p/df$ of the leaky mode for the isotropic and double anisotropic structures. Close to the plasma frequency ($f = 11$ GHz), the beam squinting of the isotropic and the anisotropic structures are comparable. However, for the anisotropic case, as frequency increases above the plasma frequency, it quickly decreases; then reaches a value that is always less than that of the isotropic slab and remains almost constant up to high frequencies.

VI. Conclusions

A broadband and low beam squint anisotropic magneto-dielectric 2D leaky-wave antenna excited by a vertical electric source has been presented. A TM_z dispersion analysis of the structure has been performed for Drude/Lorentz dispersive anisotropic and an isotropic non-dispersive grounded slabs. The analysis of the isotropic slab has shown that the pointing angle of the leaky-wave radiation is limited to the endfire region which is suppressed by the inherent radiation null of the slab at endfire. Therefore, the radiation is dominated by the space-wave which has low directivity and is incapable of beam scanning. In contrast, the anisotropic grounded slab provides a highly directive 2D leaky-wave radiation with high design flexibility. At its lower frequencies, it provides full-space conical-beam scanning while at higher frequencies, it provides fixed-beam, low-beam squint radiation (at a designable angle). As a result, this antenna may be appropriate for wide-band point-to-point communication and radar systems.

Acknowledgment

This work has partially been developed under the grant of Fundacion Seneca, frame program PCTRM 2007-2010, Spain.

References

[1] A. Oliner and D. Jackson, chap. 11 in J. Volakis (editor), *Antenna Engineering Handbook*, 4th edition, McGraw-Hill, 2007.

[2] G. V. Trentini, "Partially reflecting sheet arrays," *IEEE Trans. Antennas Propagat.*, vol. 4, no. 10, pp. 666-671, Oct. 1956.

[3] D. R. Jackson and A. A. Oliner, "A leaky-wave analysis of the high-gain printed antenna configuration," *IEEE Trans. Antennas Propagat.*, vol. 36, no. 7, pp. 905-910, July 1988.

[4] T. Zhao, D. R. Jackson, J. T. Williams, H. Y. Yang and A. A. Oliner, "2-D periodic leaky-wave antenna-part I: metal patch design," *IEEE Trans. Antennas Propagat.*, vol. 53, no. 11, pp. 3505-3514, Nov. 2005.

[5] C. A. Allen, C. Caloz, and T. Itoh, "A novel metamaterial-based two-dimensional conical-beam antenna," in *Proc. IEEE MTT-S Int. Microwave Symp. Dig.*, Fort Worth, TX, USA, pp. 305-308, June 2004.

[6] G. Lovat, P. Burghignoli, F. Capolino, D. R. Jackson, and D. R. Wilton, "Analysis of directive radiation from a line source in a metamaterial slab with low permittivity," *IEEE Trans. Antennas Propagat.*, vol. 54, no. 3, pp. 10171030, March 2006.

[7] D. Sievenpiper, L. Zhang, R. F. J. Broas, N. G. Alexopolous, and E. Yablonovitch, "High-impedance electromagnetic surfaces with a forbidden frequency band," *IEEE Trans. Microwave Theory Tech.*, vol. 47, no. 11, pp. 2059-2074, Nov. 1999.

[8] H. V. Nguyen and C. Caloz, "Anisotropic backward-wave meta-susbtrate and its application to a microstrip leaky-wave antenna," in *Proc. CNC/USNC URSI National Radio Science Meeting*, Ottawa, ON, Canada, July 2007.

[9] J. R. Mosig, "Integral equation techniques," chap. 3 in T. Itoh (editor), *Numerical Techniques for Microwave and Millimeter-wave Passive Structures*, Wiley InterSci., pp. 133-213, NY, 1989.

[10] A. B. Yakovlev, M. G. Silveirinha, O. Luukkonen, C. R. Simovskiand, I. S. Nefedov, and S. A. Tretyakov, "Characterization of the surface-waves and leaky-waves propagation on wire medium slab and mushroom structures based on local and nonlocal homogenization models," *IEEE Trans. Microwave Theory Tech.*, vol. 57, no. 11, pp. 2700-2714, Nov. 2009.

[11] S. A. Tretyakov, *Analytical Modeling in Applied Electromagnetics*, Artech House, Norwood, MA, 2003.

[12] J. B. Pendry, A. J. Holden, D. J. Robbins, and W. J. Stewart, "Magnetism from conductors and enhanced non-linear phenomena," *IEEE Trans. Microwave Theory Tech.*, vol. 47, no. 11, pp. 2075-2084, Nov. 1999.

[13] N. Marcuvitz (Ed.), *Waveguide Handbook*, chapter 8, McGraw-Hill, NY, 1951.

[14] L. B. Felsen and N. Marcuvitz, *Radiation and scattering of Waves*, Prentice-Hall/IEEE Press, NY, 1996.

[15] A. Shahvarpour, A. A. Melcon, C. Caloz, "Bandwidth enhancement and beam squint reduction of leaky modes in a uniaxially anisotropic meta-substrate," in *Proc. 2010 International Syposium on Antennas and Propagation (APS/URSI)*, Toronto, 2010.

[16] T. M. Grzegorczyk and J. R. Mosig, "Full-wave analysis containing horizontal and vertical metallizations embedded in planar multilayered media," in *IEEE Trans. Antennas Propagat.*, vol. 51, no. 11, pp. 3047-3054, Nov. 2003.

[17] J. R. Mosig, and F. E. Gardiol, chap. 3 in P. W. Hawkes (editor), *Advances in Electronics and Electron Physics*, Academic Press, NY, vol. 59, 1982.

[18] R. E. Collin, *Field Theory of Guided Waves* , 2nd edition, IEEE Press, NY, 1991.